

Si–H Bond Activation of Alkynylsilanes by Group 4 Metallocene Complexes

Martin Lamač,^{*,†} Anke Spannenberg, Wolfgang Baumann, Haijun Jiao, Christine Fischer, Sven Hansen, Perdita Arndt, and Uwe Rosenthal*

Leibniz-Institut für Katalyse e.V. an der Universität Rostock, Albert-Einstein-Strasse 29 a, 18059 Rostock, Germany

Received December 14, 2009; E-mail: uwe.rosenthal@catalysis.de; martin.lamac@jh-inst.cas.cz

Abstract: The reactivity of variously substituted alkynylsilanes toward selected group 4 metallocene complexes was investigated. Reactions of the alkynylsilanes $R^1C_2SiR^2H$ ($R^1 = SiMe_3$, $R^2 = Me$, **1**; $R^1 = SiMe_3$, $R^2 = Ph$, **2**; $R^1 = SiMe_2H$, $R^2 = Me$, **5**) with Cp_2TiMe_2 ($Cp = \eta^5$ -cyclopentadienyl) resulted, upon methyl group transfer to the silyl group, in the previously described titanocene alkyne complexes $Cp_2Ti(R^1C_2SiR^2R^3)$ ($R^1 = Me_3Si$, $R^2 = R^3 = Me$, **3**; $R^1 = HMe_2Si$, $R^2 = R^3 = Me$, **6**) or the unreported complex **4** ($R^1 = Me_3Si$, $R^2 = Ph$, $R^3 = Me$). The $Cp_2TiCl_2/n-BuLi$ system yielded alkyne complexes **6** and **7** ($R^1 = HMe_2Si$, $R^2 = Me$, $R^3 = H$); no alkyl group transfer was detected. On the other hand, reactions utilizing the $Cp_2ZrCl_2/n-BuLi$ system afforded inseparable mixtures; however, complexes of the type $Cp_2Zr[R^1C_2SiMe_2(n-Bu)]$ ($R^1 = Me_3Si$, **8**; $R^1 = HMe_2Si$, **9**) were detected. $Cp_2Hf(n-Bu)_2$ reacted with the alkynylsilanes in a diverse way, depending on the substituents of the alkyne substrate. The reaction with an excess of alkyne **1** ($R^1 = Me_3Si$, $R^2 = Me$) afforded only an intractable mixture, which contained $Me_3SiC_2SiMe_2(n-Bu)$ (**10**). Hafnacyclopentadienes **13–15** as precedented product types were obtained when alkyne **12** ($R^1 = Ph$, $R^2 = Me$) was used. In sharp contrast, the symmetrically substituted alkynes **5** ($R^1 = HMe_2Si$, $R^2 = Me$) and $H_2PhSiC_2SiPhH_2$ (**18**) yielded the hitherto unknown Si-containing metallacycles **16** and **19**. A reaction mechanism leading to these products was proposed and subsequently supported by DFT calculations. In addition, the reduction of Cp_2HfCl_2 with magnesium in THF in the presence of alkynylsilanes was shown to be an alternative route to compounds **14–16** and **19**. Presumably due to steric reasons, alkyne **1** could not form any of the product types described above. Nevertheless, it was utilized for the preparation of the PMe_3 -stabilized hafnocene alkyne complex **11**.

1. Introduction

The chemistry of group 4 metallocene alkyne complexes is well established, especially for Ti and Zr;¹ the bis(trimethylsilyl)ethyne complex of titanocene, $Cp_2Ti(\eta^2-Me_3SiC_2SiMe_3)$,^{2,1b} is the prototype in particular, which serves as a stable source

of the “free” titanocene fragment (Cp_2Ti) suitable for further reactions. Also, Zr^3 and Hf^4 constitute analogous alkyne complexes (stabilized by additional THF, pyridine, or PMe_3 ligands in the case of metallocenes bearing unsubstituted cyclopentadienyl ligands). Nevertheless, some differences in the reactivity of particular metals are evident. Notably, upon the reduction of $Cp^*_2HfCl_2$ ($Cp^* = \eta^5$ -pentamethylcyclopentadienyl) with lithium in the presence of $Me_3SiC_2SiMe_3$, an activation of both C–Si and C–H bonds was observed, and unexpected products such as metallacycle **I** (Chart 1) were isolated in addition to the simple alkyne complex.⁵ These uncommon bond activations have a potential for further development of novel synthetic tools or can help to improve the understanding of particular catalytic processes.

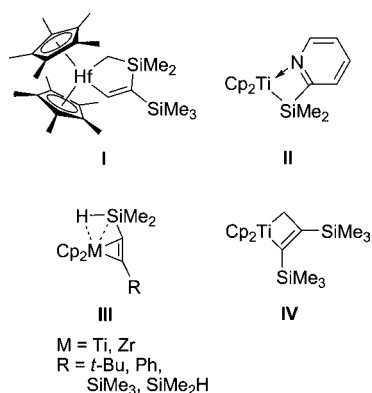
[†] On leave from the J. Heyrovský Institute of Physical Chemistry of Academy of Sciences of the Czech Republic, Dolejškova 3, 182 23 Prague 8, Czech Republic.

- (1) Review: (a) Rosenthal, U.; Burlakov, V. V. In *Titanium and Zirconium in Organic Synthesis*; Marek, I., Ed.; Wiley-VCH: Weinheim, Germany, 2002; pp 355–389. (b) Rosenthal, U.; Burlakov, V. V.; Arndt, P.; Baumann, W.; Spannenberg, A. *Organometallics* **2003**, *22*, 884.
- (2) (a) Burlakov, V. V.; Rosenthal, U.; Petrovskii, P. V.; Shur, V. B.; Vol'pin, M. E. *Organomet. Chem. USSR* **1988**, *1*, 526. (b) Burlakov, V. V.; Polyakov, A. V.; Yanovsky, A. I.; Struchkov, Y. T.; Shur, V. B.; Vol'pin, M. E.; Rosenthal, U.; Görls, H. *J. Organomet. Chem.* **1994**, *476*, 197. (c) Varga, V.; Mach, K.; Polášek, M.; Sedmera, P.; Hiller, J.; Thewalt, U.; Troyanov, S. I. *J. Organomet. Chem.* **1996**, *506*, 241.
- (3) (a) Rosenthal, U.; Ohff, A.; Michalik, M.; Görls, H.; Burlakov, V. V.; Shur, V. B. *Angew. Chem., Int. Ed. Engl.* **1993**, *32*, 1193. (b) Rosenthal, U.; Ohff, A.; Baumann, W.; Tillack, A.; Görls, H.; Burlakov, V. V.; Shur, V. B. *Z. Anorg. Allg. Chem.* **1995**, *621*, 77.
- (4) (a) Beweries, T.; Burlakov, V. V.; Bach, M. A.; Arndt, P.; Baumann, W.; Spannenberg, A.; Rosenthal, U. *Organometallics* **2007**, *26*, 247. (b) Burlakov, V. V.; Beweries, T.; Bogdanov, V. S.; Arndt, P.; Baumann, W.; Petrovskii, P. V.; Spannenberg, A.; Lyssenko, K. A.; Shur, V. B.; Rosenthal, U. *Organometallics* **2009**, *28*, 2864.

- (5) Beweries, T.; Burlakov, V. V.; Bach, M. A.; Peitz, S.; Arndt, P.; Baumann, W.; Spannenberg, A.; Rosenthal, U.; Pathak, B.; Jemmis, E. D. *Angew. Chem., Int. Ed.* **2007**, *46*, 6907.

- (6) (a) Aitken, C. T.; Harrod, J. F.; Samuel, E. *J. Organomet. Chem.* **1985**, *279*, C11. (b) Corey, J. Y.; Zhu, X.-H. *J. Organomet. Chem.* **1992**, *439*, 1. (c) Shaltout, R. M.; Corey, J. Y. *Tetrahedron* **1995**, *51*, 4309. (d) Corey, J. Y.; Zhu, X.-H.; Bedard, T. C.; Lange, L. D. *Organometallics* **1991**, *10*, 924. (e) Tilley, T. D. *Acc. Chem. Res.* **1993**, *26*, 22. (f) Gauvin, F.; Harrod, J. F.; Woo, H.-G. *Adv. Organomet. Chem.* **1998**, *42*, 363.

Chart 1



Catalyzed reactions involving organic hydrosilanes and group 4 metallocene complexes such as the dehydrogenative coupling to oligo- and polysilanes,⁶ or hydrosilylation of unsaturated organic substrates (alkenes,⁷ alkynes,⁸ imines,⁹ ketones,¹⁰ pyridines¹¹) are well documented. Metallocene silyl hydride complexes were postulated as intermediates in some of these processes. Owing to the rather high reactivity of the M–Si bond, which can undergo an insertion to unsaturated bonds,¹² or σ -bond metathesis with other Si–H or even C–H bonds,^{13,6e} relatively few metallocene silyl complexes have been isolated.¹⁴ Complexes containing the Cp₂M–SiR₃ fragment were prepared, e.g., by the reaction of Cp₂MCl₂ (M = Ti, Zr, Hf) with Al(SiMe₃)₃·OEt₂¹⁵ or LiSiR₃,^{12a,14} to provide chloro silyl or disilyl substituted metallocenes. Another approach utilized the reaction of Ph₂RSiH (R = H, Ph) with alkene complexes of Cp₂M (M = Zr, Hf) or with Cp₂Ti(PMe₃)₂ to yield the metallocene silyl hydride complexes Cp₂M(H)SiPh₂R (stabilized by the coordination of an additional PMe₃ ligand).^{7b,16,17} As already mentioned, metallocene silyl complexes may undergo

σ -bond metathesis with other silanes (primary or secondary), which is an alternative route to other silyl complexes.¹³ Metallocene silyl complexes were also isolated as intermediates in the catalytic dehydrocoupling of silanes or hydrosilylation reactions. In both processes, Cp₂MMe₂ (M = Ti, Zr) were used as precatalysts, which reacted with primary or secondary silanes. The structural motifs, which were observed, comprise Ti(III) dimers bridged by the hydride anion or the hydrosilyl moiety,¹⁸ doubly hydride bridged silyl Zr(IV) dimers,¹⁹ or paramagnetic Ti(III) monomers stabilized by a pyridine or tertiary phosphine ligand.^{11,20} Such reactions are almost fully restricted to primary and secondary silanes, while tertiary derivatives are often claimed to be inert. However, the sole example of a tertiary silyl Ti(III) complex (**II**; Chart 1) was prepared in a similar manner from Cp₂TiMe₂ and 2 equiv of 2-(dimethylsilyl)pyridine by Harrod and co-workers.²¹

Several complexes of titanium and zirconium with alkynes bearing dimethylsilyl groups (**III**; Chart 1)²² were previously prepared either by the alkyne-exchange reaction in the complexes Cp₂M(η^2 -Me₃SiC₂SiMe₃) (M = Ti, Zr) with the corresponding alkynylsilane or by the reduction of Cp₂MCl₂ with magnesium in THF in the presence of the alkynylsilane. It was shown that an agostic two-electron three-center Si–H–M interaction involving the hydrosilyl group is present, while the coordinated alkyne fragment adopts the trans configuration. Complex **III** (M = Ti, R = SiMe₂H; Chart 1) has been also described by theoretical calculations to have a d² system with comparable back-donating strengths of the alkyne and the Si–H bond.²³ The competition between the alkyne and the Si–H moiety for coordination to the metal center is manifested both structurally and electronically. Such complexes resemble an intramolecularly stabilized intermediate of the alkyne hydrosilylation reaction and therefore serve as valuable model compounds for such processes. Analogous complexes have not yet been reported for hafnium.

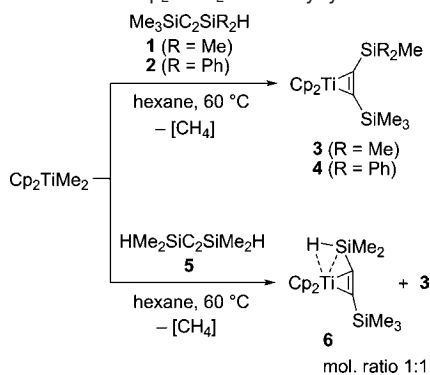
In this study, we describe the reactivity of selected group 4 metallocene complexes with various alkynylsilanes, stressing the differences arising from the different nature of particular metals and metallocene sources and from steric demands of the alkyne substrates. For the novel hafnium complexes, we present detailed density functional investigations concerning the reaction mechanism of their formation.

2. Results and Discussion

To explore the interaction of group 4 metallocene alkyl complexes with alkynyl hydrosilanes, we performed a series of reactions using Cp₂TiMe₂, Cp₂ZrMe₂, Cp₂Hf(*n*-Bu)₂, or in situ generated dialkyl complexes from the Cp₂TiCl₂/*n*-BuLi or

- (7) (a) Harrod, J. F.; Yun, S. S. *Organometallics* **1987**, *6*, 1381. (b) Takahashi, T.; Hasegawa, M.; Suzuki, N.; Saburi, M.; Rousset, C. J.; Fanwick, P. E.; Negishi, E. *J. Am. Chem. Soc.* **1991**, *113*, 8564. (c) Corey, J. Y.; Zhu, X.-H. *Organometallics* **1992**, *11*, 672. (d) Kesti, M. R.; Waymouth, R. M. *Organometallics* **1992**, *11*, 1095.
- (8) Takahashi, T.; Bao, F.; Gao, G.; Ogasawara, M. *Org. Lett.* **2003**, *5*, 3479.
- (9) (a) Verdagner, X.; Lange, U. E. W.; Reding, M. T.; Buchwald, S. L. *J. Am. Chem. Soc.* **1996**, *118*, 6784. (b) Tillack, A.; Lefeber, C.; Peulecke, N.; Thomas, D.; Rosenthal, U. *Tetrahedron Lett.* **1997**, *38*, 1533.
- (10) Halterman, R. L.; Ramsey, T. M.; Chen, Z. *J. Org. Chem.* **1994**, *59*, 2642.
- (11) (a) Hao, L.; Harrod, J. F.; Lebusis, A.-M.; Mu, Y.; Shu, R.; Samuel, E.; Woo, H.-G. *Angew. Chem., Int. Ed.* **1998**, *37*, 3126. (b) Harrod, J. F.; Shu, R.; Woo, H.-G.; Samuel, E. *Can. J. Chem.* **2001**, *79*, 1075.
- (12) (a) Campion, B. K.; Falk, J.; Tilley, T. D. *J. Am. Chem. Soc.* **1987**, *109*, 2049. (b) Elsner, F. H.; Tilley, T. D.; Rheingold, A. L.; Geib, S. J. *J. Organomet. Chem.* **1988**, *358*, 169.
- (13) (a) Woo, H.-G.; Tilley, T. D. *J. Am. Chem. Soc.* **1989**, *111*, 3757. (b) Woo, H.-G.; Tilley, T. D. *J. Am. Chem. Soc.* **1989**, *111*, 8043. (c) Woo, H.-G.; Heyn, R. H.; Tilley, T. D. *J. Am. Chem. Soc.* **1992**, *114*, 5698. (d) Woo, H.-G.; Walzer, J. F.; Tilley, T. D. *J. Am. Chem. Soc.* **1992**, *114*, 7047. (e) Casty, G. L.; Lugmair, C. G.; Radu, N. S.; Tilley, T. D.; Walzer, J. F.; Zargarian, D. *Organometallics* **1997**, *16*, 8. (f) Sadow, A. D.; Tilley, T. D. *J. Am. Chem. Soc.* **2002**, *124*, 6814. (g) Sadow, A. D.; Tilley, T. D. *J. Am. Chem. Soc.* **2003**, *125*, 9462.
- (14) Nevertheless, compounds with group 4 metal–silicon bonds were reported as early as the 1960s: Cardin, D. J.; Keppie, S. A.; Kingston, B. M.; Lappert, M. F. *Chem. Commun.* **1967**, 1035. For other examples, see refs 11–21.
- (15) (a) Röscher, L.; Altnau, G.; Erb, W.; Pickardt, J.; Bruncks, N. *J. Organomet. Chem.* **1980**, *197*, 51. (b) Tilley, T. D. *Organometallics* **1985**, *4*, 1452.
- (16) Kreuzer, K. A.; Fischer, R. A.; Davis, W. M.; Spaltenstein, E.; Buchwald, S. L. *Organometallics* **1991**, *10*, 4031.

- (17) Spaltenstein, E.; Palma, P.; Kreuzer, K. A.; Willoughby, C. A.; Davis, W. M.; Buchwald, S. L. *J. Am. Chem. Soc.* **1994**, *116*, 10308.
- (18) Aitken, C. T.; Harrod, J. T.; Samuel, E. *J. Am. Chem. Soc.* **1986**, *108*, 4059.
- (19) (a) Aitken, C. T.; Harrod, J. T.; Samuel, E. *Can. J. Chem.* **1986**, *64*, 1677. (b) Mu, Y.; Aitken, C.; Cote, B.; Harrod, J. F.; Samuel, E. *Can. J. Chem.* **1991**, *69*, 264.
- (20) Samuel, E.; Mu, Y.; Harrod, J. F.; Dromzee, Y.; Jeannin, Y. *J. Am. Chem. Soc.* **1990**, *112*, 3435.
- (21) Hao, L.; Woo, H.-G.; Lebusis, A.-M.; Samuel, E.; Harrod, J. F. *Chem. Commun.* **1998**, 2013.
- (22) (a) Ohff, A.; Kosse, P.; Baumann, W.; Tillack, A.; Kempe, R.; Görls, H.; Burlakov, V. V.; Rosenthal, U. *J. Am. Chem. Soc.* **1995**, *117*, 10399. (b) Peulecke, N.; Ohff, A.; Kosse, P.; Tillack, A.; Spannenberg, A.; Kempe, R.; Baumann, W.; Burlakov, V. V.; Rosenthal, U. *Chem. Eur. J.* **1998**, *4*, 1852.
- (23) Fan, M.-F.; Lin, Z. *Organometallics* **1997**, *16*, 494.

Scheme 1. Reactions of Cp₂TiMe₂ with Alkynylsilanes

Cp₂ZrCl₂/*n*-BuLi system. We initially anticipated a reaction between Si–H and the alkyl substituent on the metal which, upon release of the corresponding alkane, would result in the formation of a M–Si bond. Such a mechanism leading to metallocene silyl complexes was preceded, as mentioned above.^{18–20} In the case of alkynes substituted symmetrically with two Si–H-containing groups, such reactions could yield interesting metallacycles with silicon atoms and the C≡C triple bond incorporated in the five-membered ring.²⁴ On the other hand, observations on the reactivity of Cp₂TiMe₂ with various alkynes under thermolytic conditions by Petasis²⁵ and Doxsee²⁶ could also suggest different reaction pathways for this particular substrate. As a representative example, Cp₂TiMe₂ with an excess of Me₃SiC₂SiMe₃ gives cleanly, upon heating in benzene to 80 °C in the dark, the corresponding titanacyclobutene complex (**IV**; Chart 1). The reaction proceeds presumably via the reactive methylidenetitanocene intermediate.

2.1. Reactions of Cp₂MMe₂ (M = Ti, Zr). Under our experimental conditions, no products such as silyl complexes or titanacyclobutenes were obtained or observed during the reaction. Instead, methyl group transfer to the Si atom occurred and the corresponding metallocene alkyne complex was formed. Thus, the reaction of Cp₂TiMe₂ with 1 equiv of Me₃SiC₂SiMe₂H (**1**; Scheme 1) in *n*-hexane at 60 °C afforded the known complex Cp₂Ti(η²-Me₃SiC₂SiMe₃) (**3**). In a similar fashion, using Me₃SiC₂SiPh₂H (**2**), the previously unknown alkyne complex **4** was isolated. This compound could be further recrystallized from *n*-hexane to yield air- and moisture-sensitive amber crystals (63%), suitable also for an X-ray structural analysis. The molecular structure of **4** (Figure 1) reveals an expected mode of interaction between the bent-metallocene core and the substituted alkyne ligand. The observed structural parameters are comparable to those found in compound **3**,^{1b} suggesting a titanacyclopentene structure. Also, NMR and IR spectroscopic data of **4** are in accordance with the formulated structure and resemble those of **3**.²

When a stoichiometric amount of the symmetrical alkyne HMe₂SiC₂SiMe₂H (**5**) was used, a mixture of compounds **3** and **6** in a ca. 1:1 molar ratio was obtained. Compound **6** with one SiMe₂H group participating in the agostic interaction with the metal center was also previously described.²² Concerning the mechanism of formation of the previously described products,

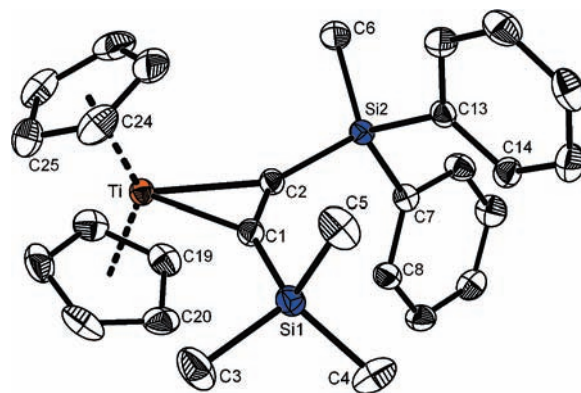
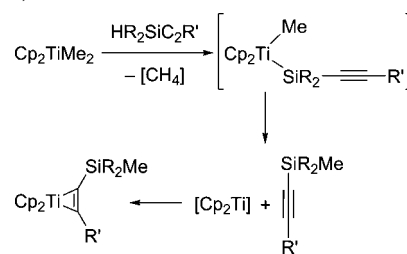


Figure 1. Molecular structure of compound **4**. Hydrogen atoms are omitted for clarity; thermal ellipsoids correspond to the 30% probability level. Selected bond lengths (Å) and angles (deg): Ti–C1 = 2.1077(14), Ti–C2 = 2.1155(13), C1–C2 = 1.290(2), C1–Si1 = 1.8440(15), C2–Si2 = 1.8366(14); C1–Ti–C2 = 35.56(5), Si1–C1–C2 = 145.07(12), C1–C2–Si2 = 139.65(12).

Scheme 2. Suggested Reaction Mechanism for the Formation of Products **3**, **4**, and **6**

we suggest a stepwise process (Scheme 2), which includes the σ -bond metathesis of Si–H and Ti–C bonds to give the silyl complex. Subsequently, a reductive elimination takes place,²⁷ followed by the coordination of the free alkylated alkynylsilane. However, we do not have enough experimental evidence for the formation of any intermediates. It is noteworthy that, when an excess of the alkynes was used, the reactions yielded only intractable mixtures containing probably also paramagnetic species that we could not identify.

Reactions similar to those previously described using the zirconium analogue Cp₂ZrMe₂ did not proceed at all. Only after prolonged reaction time at the reflux temperature, the product of partial hydrolysis (by traces of moisture), [Cp₂Zr(Me)]₂O,²⁸ was detected in the reaction mixture by NMR, together with the unchanged starting complex. Due to such a significantly lower reactivity of Cp₂ZrMe₂, the corresponding hafnium derivative was not tested in this reaction.

2.2. Reactions of Cp₂MCl₂/*n*-BuLi Systems (M = Ti, Zr). Additionally, metallocene complexes bearing *n*-butyl groups were probed as substrates. In the case of Ti and Zr, such Cp₂M(*n*-Bu)₂ species are stable only at low temperatures. They are generated in situ from Cp₂MCl₂ and 2 equiv of *n*-BuLi at –78 °C. Complicated decomposition pathways of the zirconium derivative (also known as the Negishi reagent) with increasing temperature were described in detail by Harrod et al.²⁹ In a

(24) An alternative approach leading to such compounds will be described elsewhere: Lamač, M.; Spannenberg, A.; Jiao, H.; Hansen, S.; Baumann, W.; Arndt, P.; Rosenthal, U. *Angew. Chem., Int. Ed.*, in press.

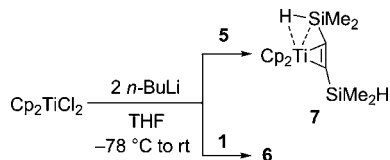
(25) Petasis, N. A.; Fu, D.-K. *Organometallics* **1993**, *12*, 3776.

(26) Doxsee, K. M.; Juliette, J. J.; Mouser, J. K. M.; Zientara, K. *Organometallics* **1993**, *12*, 4682.

(27) The reductive elimination of silyl groups from titanocene was recently reported: Zirngast, M.; Flörke, U.; Baumgartner, J.; Marschner, C. *Chem. Commun.* **2009**, 5538.

(28) The product was identified by NMR spectroscopy. For references, see: Marsella, J. A.; Huffman, J. C.; Folting, K.; Caulton, K. G. *Inorg. Chim. Acta* **1985**, *96*, 161.

(29) Dioumaev, V. K.; Harrod, J. F. *Organometallics* **1997**, *16*, 1452.

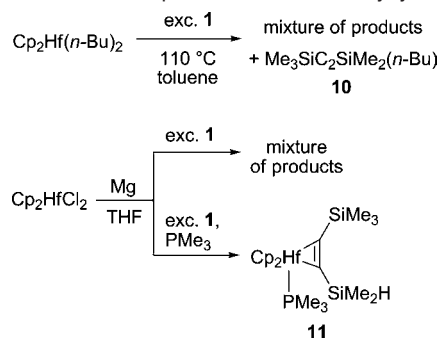
Scheme 3. Reactions of the $\text{Cp}_2\text{TiCl}_2/n\text{-BuLi}$ System with Alkynylsilanes

simplified conception, the zirconocene 1-butene complex is formed, which can easily generate the “free” zirconocene fragment in reactions with various substrates. The titanium analogue behaves similarly but is even less thermally stable, which corresponds with our observations.

The $\text{Cp}_2\text{TiCl}_2/n\text{-BuLi}$ system in the presence of stoichiometric amounts of alkynes **1** and **5** produced the known complexes **6** and **7**, respectively, upon warming the mixtures of reagents to room temperature (Scheme 3). The “ Cp_2Ti ” species was probably generated already at low temperature and immediately stabilized by coordination of the alkynes. On the other hand, the $\text{Cp}_2\text{ZrCl}_2/n\text{-BuLi}$ system facilitated the *n*-butyl group transfer to alkynylsilanes **1** and **5**. Unfortunately, the reactions using in situ generated dialkyl complexes (in particular the zirconocene system) produced various amounts of unidentified byproducts, arguably as a result of multiple decomposition pathways of the metallocene precursor. The isolation of analytically pure samples of the described products was impossible because these compounds (as well as the impurities) were oily solids that were extremely soluble, even in cold hydrocarbon solvents. In general, alkyne complexes of the type $\text{Cp}_2\text{Zr}[\text{R}^1\text{C}_2\text{SiMe}_2(n\text{-Bu})]$ ($\text{R}^1 = \text{Me}_3\text{Si}$, **8**; $\text{R}^1 = \text{HMe}_2\text{Si}$, **9**), in which the *n*-butyl group was present at one Si atom, were major components of the reaction mixtures, as concluded from NMR spectra and the HR ESI-MS analysis (see the Supporting Information for details). Also, free alkynes **10** and **17** (see below), which resulted from the *n*-butyl group transfer from $\text{Cp}_2\text{Zr}(n\text{-Bu})_2$ to one or both silicon atoms of the substrate **1** or **5**, were later identified in the mixtures by comparison of their spectral data. A similar formal transfer of the *n*-butyl group from the in situ generated $\text{Cp}_2\text{Zr}(n\text{-Bu})_2$ to Ph_2SiH_2 was previously reported.^{7b} Formal hydrosilylation of 1-butene in the coordination sphere of Zr and subsequent coordination of the alkyne to the metallocene fragment or a consecutive process beginning with the Zr–C and Si–H σ -bond metathesis¹³ involving the *n*-butyl substituent are both possible explanations of the reaction mechanism.

2.3. Reactions of “ Cp_2Hf ” Sources. In contrast to the Ti and Zr *n*-butyl complexes, the hafnium analogue $\text{Cp}_2\text{Hf}(n\text{-Bu})_2$ can be prepared as a defined stable solid material.^{4b} Owing to its enhanced stability, higher temperatures are necessary to initiate the reaction. In the case of this metallocene source, structures of the reaction products turned out to be dependent on the substitution of the alkynylsilane used, particularly on steric properties of the substituents present on silicon. To demonstrate these differences, we utilized an even broader set of alkynylsilanes. In contrast to the previous experiments, using an excess (2.5–3 mol equiv) of the corresponding alkynylsilane proved to be essential to obtain well-defined products, as is shown below.

Reaction of $\text{Cp}_2\text{Hf}(n\text{-Bu})_2$ with either 1 or 3 molar equiv of **1** in toluene at 110 °C gave only mixtures of unidentified decomposition products of the hafnocene precursor (Scheme 4). The sole identified compound was the yet unreported product of the *n*-butyl group transfer to the silyl group, alkyne **10**. In an additional experiment, a slight excess of $\text{Cp}_2\text{Hf}(n\text{-Bu})_2$ with

Scheme 4. Reactions of “ Cp_2Hf ” Sources with Alkynylsilane **1**

respect to **1** was used, and compound **10** was isolated for characterization purposes from the mixture upon hydrolysis of hafnium byproduct and subsequent chromatography on alumina.

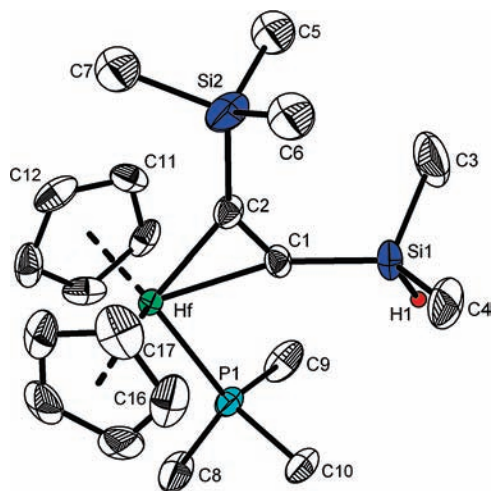
The reduction of Cp_2HfCl_2 with magnesium in the presence of **1** (Scheme 4) led also to an intractable mixture, as was the case when $\text{Me}_3\text{SiC}_2\text{SiMe}_3$ was employed.^{4a} However, the presence of the alkyne complex $\text{Cp}_2\text{Hf}(\text{HMe}_2\text{SiC}_2\text{SiMe}_3)$ was detected in the mixture by EI-MS.³⁰ Unfortunately, we were not able to isolate this compound without further stabilizing ligands. When the reduction was performed in the presence of PMe_3 together with **1**, the phosphine-stabilized alkyne complex **11** was formed. A highly air- and moisture-sensitive orange crystalline material was isolated and characterized. Notably, a mixture of two isomers (molar ratio ca. 12:1) with respect to the mutual orientation of the alkyne moiety and the phosphine ligand is observed in solution by NMR spectroscopy. However, NMR as well as IR spectra show expected features for the major isomer, such as high-field-shifted doublets of the alkyne carbon atoms in ¹³C spectra (179.7 and 216.4 ppm, respectively), a singlet at –7.4 ppm in the ³¹P spectrum, and bands attributable to the Si–H stretch (2086 cm^{-1}) and the coordinated triple bond stretch (1562 cm^{-1}) in the IR spectrum. The solid-state structure of complex **11** (the preferentially crystallized major isomer) was determined by X-ray diffraction (Figure 2). It reveals a structure analogous to the known complex of $\text{Me}_3\text{SiC}_2\text{SiMe}_3$.^{4a} The less sterically demanding dimethylsilyl group is expectedly oriented toward the PMe_3 ligand, while no further interaction of the Si–H bond with the coordinatively saturated metallocene core could be found.

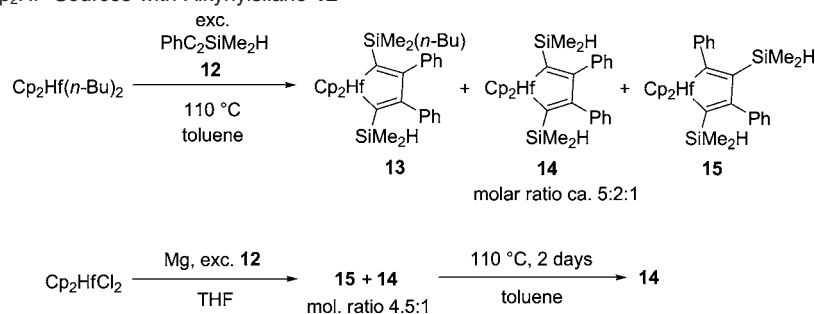
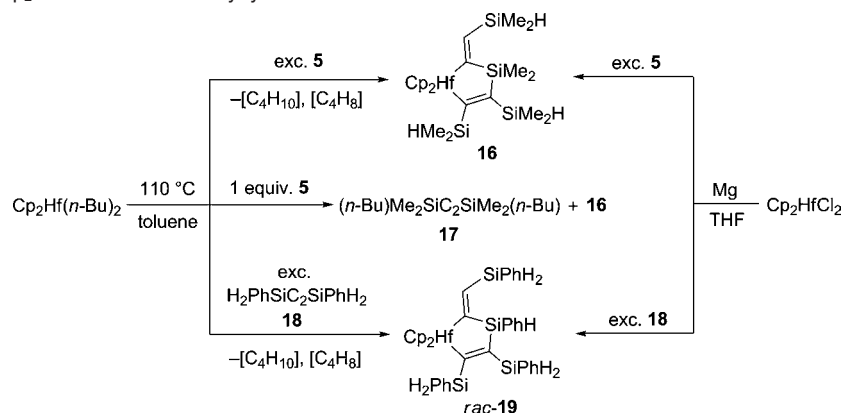
An experiment performed under conditions analogous to those previously described starting with $\text{Cp}_2\text{Hf}(n\text{-Bu})_2$ and alkyne $\text{PhC}_2\text{SiMe}_2\text{H}$ (**12**) yielded a mixture of hafnacyclopentadienes **13**–**15** in the molar ratio ca. 5:2:1 (Scheme 5). By recrystallization, we were only able to obtain a mixture of compounds **13** and **14**. Hafnacyclopentadienes of this kind are known product types of reactions between hafnocene alkyl complexes or in situ formed “free” hafnocene and certain alkynes.^{31,4a} Analogous structures were also found for Ti and Zr with alkyne **12** as the substrate.^{22b,32} Notably, the dominant product of the reaction using $\text{Cp}_2\text{Hf}(n\text{-Bu})_2$ contains the *n*-butyl group attached to one of the Si atoms as a consequence of the transfer from the hafnocene precursor. NMR spectra are consistent with the

(30) See the Supporting Information for details.

(31) (a) Atwood, J. L.; Hunter, W. E.; Rausch, M. D. *J. Am. Chem. Soc.* **1976**, *98*, 2454. (b) Sabada, M. B.; Faron, M. F.; Zarate, E. A.; Youngs, W. J. *J. Organomet. Chem.* **1988**, *338*, 347. (c) Yousaf, S. M.; Faron, M. F.; Shively, R. J.; Youngs, W. J. *J. Organomet. Chem.* **1989**, *363*, 281.

(32) Kempe, R.; Spannenberg, A.; Kosse, P.; Peulecke, N.; Rosenthal, U. *Z. Kristallogr.-New Cryst. Struct.* **1998**, *213*, 789.



Scheme 5. Reactions of “Cp₂Hf” Sources with Alkynylsilane **12**Scheme 6. Reactions of “Cp₂Hf” Sources with Alkynylsilanes **5** and **18**

anism leading to this structure is undoubtedly different. In the case of compound **19**, the racemic mixture of enantiomers gave rise to a structure conformable with the centrosymmetric $P\bar{1}$ space group. The C1–C2 bond in both complexes clearly has a double-bond character, which is demonstrated by the lengths of 1.362(3) Å (for **16**) and 1.360(4) Å (for **19**), respectively. The same is true of the exocyclic C3–C4 bond (1.351(4) Å for

16, 1.346(5) Å for **19**), which adopts the *E* configuration with the SiMe₂H or SiPhH₂ group pointing out from the metallocene core. Other bonds fall into the range typical for single bonds of the corresponding type. For example, distances between hafnium and the ring carbons C1 and C3 are 2.251(2) and 2.225(3) Å

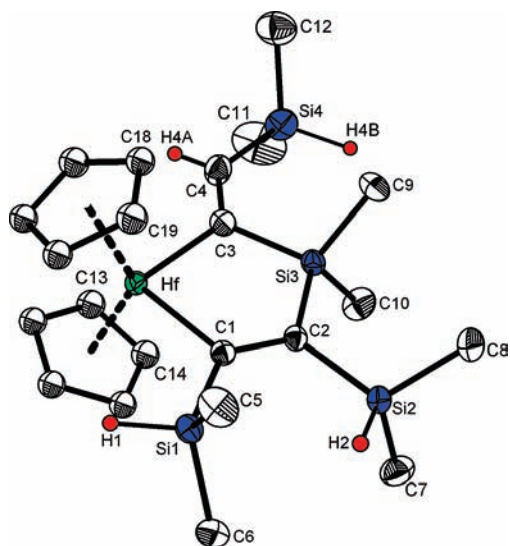


Figure 3. Molecular structure of compound **16**. Only one position of the disordered cyclopentadienyl rings is shown. Hydrogen atoms are omitted for clarity, except for Si–H protons (H1, H2, H4B), and H4A. Thermal ellipsoids correspond to the 30% probability level. Selected bond lengths (Å) and angles (deg): Hf–C1 = 2.251(2), Hf–C3 = 2.225(3), C1–C2 = 1.362(3), C2–Si3 = 1.892(3), C3–Si3 = 1.880(3), C3–C4 = 1.351(4); C1–Hf–C3 = 91.08(10), Hf–C1–C2 = 115.1(2), C1–C2–Si3 = 120.0(2), C2–Si3–C3 = 107.37(12), Hf–C3–Si3 = 106.29(14), Hf–C3–C4 = 131.1(2).

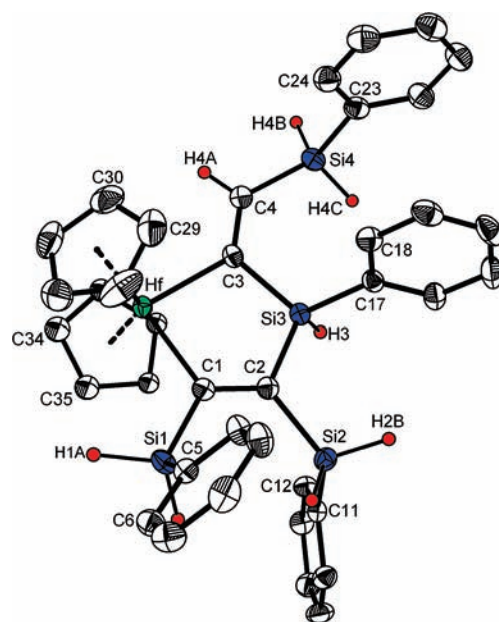
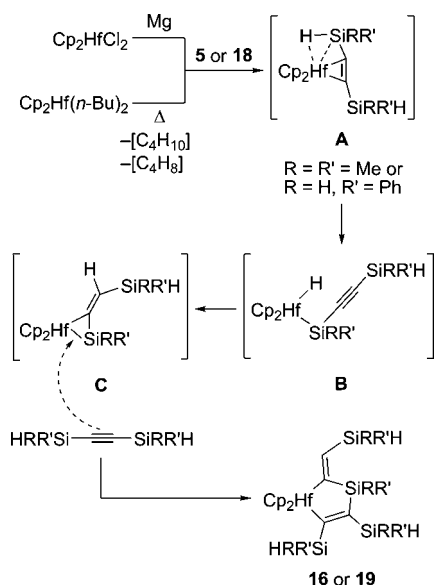


Figure 4. Molecular structure of *rac*-**19** (the *S* enantiomer is shown). Only one position of the disordered Cp ring C34–C38 is shown. Hydrogen atoms are omitted for clarity, except for Si–H protons (H1A, H1B, H2A, H2B, H3, H4B, H4C) and H4A. Thermal ellipsoids correspond to the 30% probability level. Selected bond lengths (Å) and angles (deg): Hf–C1 = 2.253(3), Hf–C3 = 2.240(3), C1–C2 = 1.360(4), C2–Si3 = 1.886(3), C3–Si3 = 1.878(3), C3–C4 = 1.346(5); C1–Hf–C3 = 88.90(11), Hf–C1–C2 = 116.9(2), C1–C2–Si3 = 118.7(2), C2–Si3–C3 = 107.04(13), Hf–C3–Si3 = 106.8(2), Hf–C3–C4 = 130.2(2).

Scheme 7. Proposed Mechanism of Formation of Compounds **16** and **19**

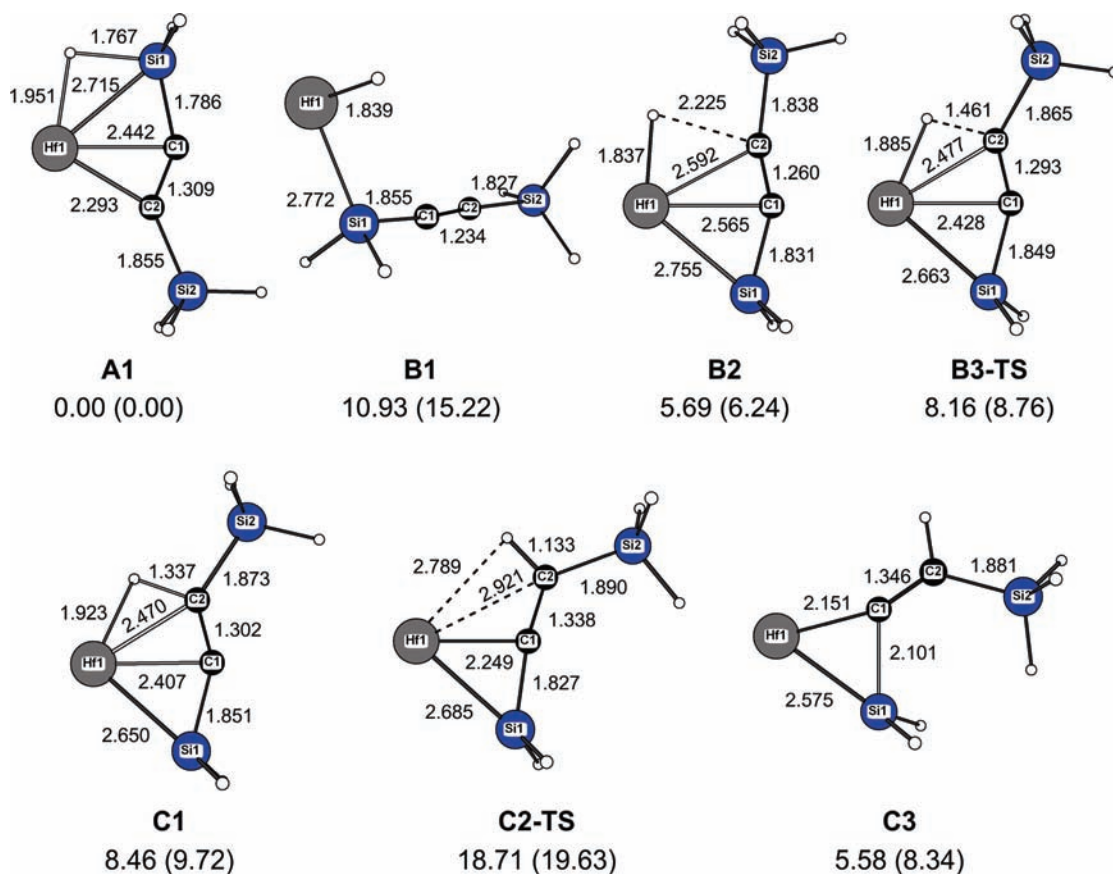
for **16** and 2.253(3) and 2.240(3) Å for **19**, respectively, which is comparable to distances found in **I**.⁵ The five-membered ring Hf–C1–C2–Si3–C3 in **16** is nearly planar (mean deviation of 0.02 Å), and also the C4 sp^2 carbon atom and silicon atoms Si1, Si2, and Si4 do not markedly deviate from this plane. Only the SiMe₂H group on C2 is slightly bent out from the plane of the metallacycle; the torsion angle Hf–C1–C2–Si2 is –

172.82(12)°. The five-membered ring Hf–C1–C2–Si3–C3 in **19** is slightly deformed (e.g., the torsion angles C1–Hf–C3–Si3 and Hf–C1–C2–Si3 are 11.0(1) and 8.7(3)°, respectively). Pendant phenyl substituents of SiPh₂ groups are twisted from the plane of the central five-membered ring in order to meet steric demands. Phenyl rings C17–C22 and C23–C28 are involved in a weak intramolecular π – π interaction (distance of ring centroids 3.93 Å, dihedral angle between ring planes 14.51°, slip angles³⁴ 31.68, 21.61°), while phenyl groups C5–C10 of two adjacent molecules in the crystal structure interact similarly, being in a virtually coplanar orientation (distance of ring centroids 3.98 Å, slip angle 30.22°).

3. Mechanistic Considerations

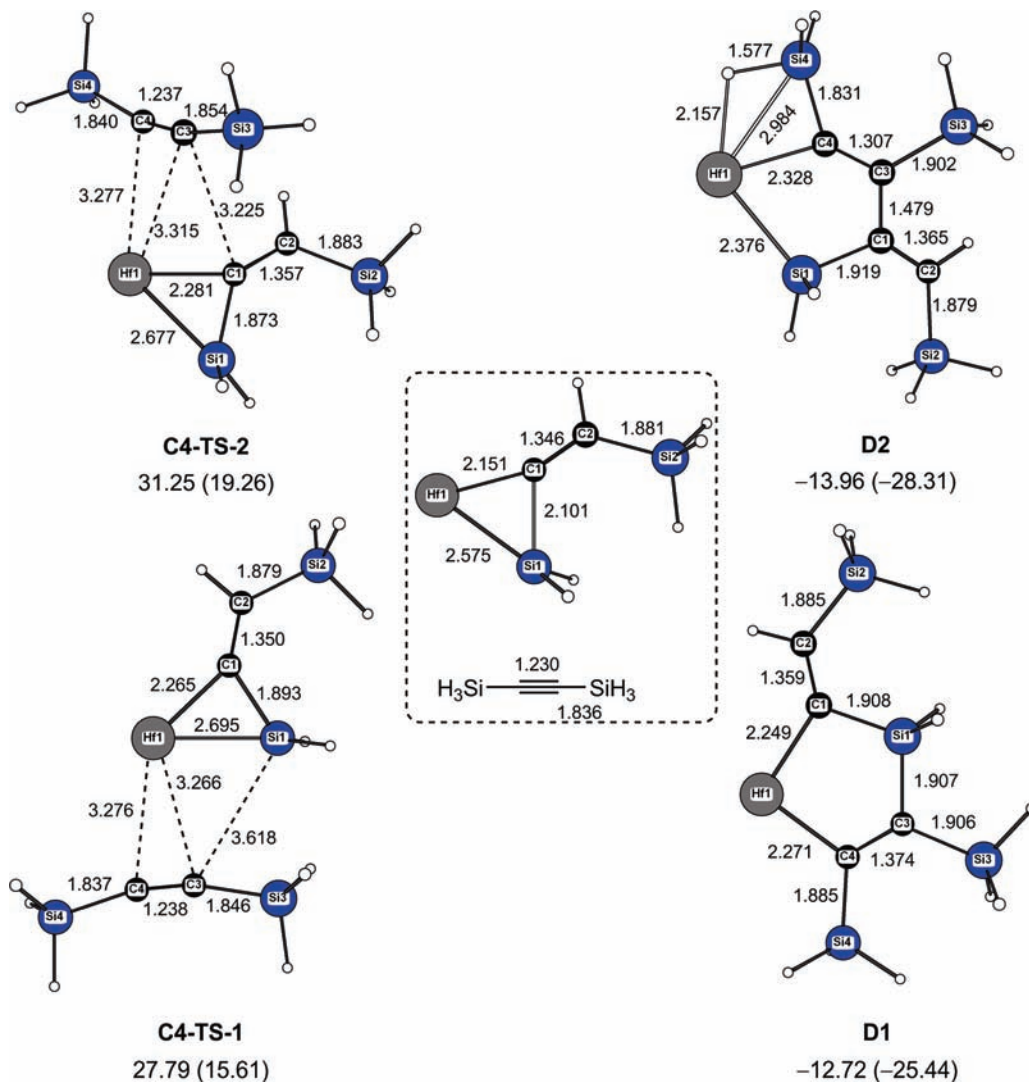
Concerning the mechanism of formation of metallacycles **16** and **19**, we suggest that both $\text{Cp}_2\text{Hf}(n\text{-Bu})_2$ (at 110 °C) and the $\text{Cp}_2\text{HfCl}_2/\text{Mg}$ system generate the “free” hafnocene that is immediately stabilized by the coordination of the corresponding alkyne. The resulting metallocene alkyne complex could be similar to those reported²² for Ti and Zr with the trans configuration of the coordinated alkyne and an agostic Si–H–M interaction (**A** in Scheme 7). $\text{Cp}_2\text{Hf}(n\text{-Bu})_2$ is expected to eliminate *n*-butane under reaction conditions upon the formation of an alkene complex. This can, indeed, undergo the alkene–alkyne exchange, affording intermediate **A**. At this point, also the concurrent process—a formal hydrosilylation of 1-butene—could take place, leading to the observed side product **17**.³⁵

Subsequent activation of the Si–H bond in **A** is a prerequisite for the reorganization leading to the main product. In this

Scheme 8. BP86 Computed Bond Distances (Å), Gibbs Free Energies (ΔG , kcal/mol), and Enthalpies (ΔH , kcal/mol, in Parentheses) for the Isomerization Reaction of the Suggested Intermediate **A** to **C**^a

^a See Scheme 7. Cyclopentadienyl rings on Hf were omitted for simplicity.

Scheme 9. BP86 Computed Bond Distances (Å), Gibbs Free Energies (ΔG , kcal/mol), and Enthalpies (ΔH , kcal/mol, in Parentheses) for the Insertion Reaction of the Second Molecule of the Alkyne Substrate to Intermediate **C**^a



^a See Scheme 7. Cyclopentadienyl rings on Hf were omitted for simplicity.

manner, a silyl hydride complex (**B**) should be formed, which could transform into a hafnasilacyclopropane structure (**C**). We also cannot exclude the direct formation of intermediate **B** by the oxidative addition of alkynylsilane to the “free” metallocene species. A structural motif similar to that of **C** was observed in the structure of the ruthenium complex reported by Jones³⁶ or in the species proposed by Mori and co-workers as an intermediate during reactions of Cp_2ZrCl_2 with Me_2PhSiLi .³⁷ Under these conditions, the presence of a zirconium–silene complex (or silazirconacyclopropane) was anticipated and such ideas were supported by further reactions

with alkynes that yielded silazirconacyclopentenes via insertion of the alkyne into the Zr–Si bond. However, these compounds were observed only spectroscopically and the mechanism was deduced from products of the subsequent hydrolysis, which yielded the correspondingly substituted vinylsilanes. Obviously, a similar process of insertion could lead in our case to the formation of the isolated products **16** and **19**. The in situ NMR monitoring (toluene-*d*₈, 100 °C, 5 min interval) of the reaction leading to **16** revealed the formation of one major intermediate with a resonance for Cp protons at 4.87 ppm. According to Mori et al., the zirconocene silene complex exhibited a signal for Cp protons at lower chemical shifts compared to the zirconacyclopentene product.^{37a} On the basis of this analogy, silene complex **C** could be present in our system. The concentration of the observed species culminated after ca. 40 min, when it reached approximately 30% of the sum of molar concentrations of the reactant and the product. Then the signal gradually dropped away as the product was formed. In addition, a small signal at –3.94 ppm (approximately 5% intensity of the latter signal) was present, which can be explained by the silyl group proton in an agostic interaction with the metal possibly belonging to

(34) Angles between centroid–centroid vector and normal to the respective plane.

(35) Metathesis of σ -bonds involving the starting $\text{Cp}_2\text{Hf}(n\text{-Bu})_2$ is another possible pathway. Such transfer of a methyl group from Hf complexes to PhSiH_3 has also been reported: Sadow, A. D.; Tilley, T. D. *Organometallics* **2003**, *22*, 3577.

(36) Yin, J.; Klosin, J.; Abboud, K. A.; Jones, W. M. *J. Am. Chem. Soc.* **1995**, *117*, 3298.

(37) (a) Mori, M.; Kuroda, S.; Dekura, F. *J. Am. Chem. Soc.* **1999**, *121*, 5591. (b) Kuroda, S.; Dekura, F.; Sato, Y.; Mori, M. *J. Am. Chem. Soc.* **2001**, *123*, 4139. (c) Mori, M. *Top. Organomet. Chem.* **2005**, *10*, 41.

Table 1. Crystallographic Data for **4**, **11**, **16**, and **19**

	4	11	16	<i>rac</i> - 19
formula	C ₂₈ H ₃₂ Si ₂ Ti	C ₂₀ H ₃₅ HfPSi ₂	C ₂₂ H ₃₈ HfSi ₄	C ₃₈ H ₃₈ HfSi ₄
<i>M_r</i>	472.62	541.12	593.37	785.53
cryst syst	triclinic	monoclinic	monoclinic	triclinic
space group	<i>P</i> $\bar{1}$	<i>P</i> 2 ₁ / <i>c</i>	<i>C</i> 2/ <i>c</i>	<i>P</i> $\bar{1}$
<i>T</i> (K)	200(2)	200(2)	200(2)	200(2)
<i>a</i> (Å)	8.5394(4)	16.8109(5)	32.0481(10)	8.1828(2)
<i>b</i> (Å)	10.3251(5)	10.2196(3)	9.1762(2)	10.4511(3)
<i>c</i> (Å)	16.5699(8)	14.9047(5)	20.1421(7)	20.5913(6)
α (deg)	94.324(4)	90	90	88.056(2)
β (deg)	101.046(3)	109.929(2)	113.035(2)	84.173(2)
γ (deg)	114.318(3)	90	90	80.283(2)
<i>V</i> (Å ³)	1287.09(11)	2407.30(13)	5451.1(3)	1726.47(9)
<i>Z</i>	2	4	8	2
<i>D</i> _{calc} (g cm ⁻³)	1.219	1.493	1.446	1.511
μ (Mo K α) (mm ⁻¹)	0.44	4.50	4.01	3.19
cryst size (mm)	0.37 × 0.34 × 0.12	0.20 × 0.15 × 0.08	0.47 × 0.20 × 0.17	0.42 × 0.23 × 0.03
color, habit	yellow, prism	orange, prism	yellow, prism	yellow, plate
transmissn coeff	0.809–0.922	0.431–0.735	0.316–0.576	0.520–0.926
no. of total/unique rflns	24 788/6939	31 646/4476	40 215/5776	26 806/7322
no. of obsd rflns (<i>I</i> > 2 σ (<i>I</i>))	4795	3158	4264	6175
<i>R</i> _{int} (%)	2.75	7.65	2.83	3.42
no. of params	284	184	207	366
<i>R</i> 1 (<i>I</i> > 2 σ (<i>I</i>)) (%)	3.22	3.63	1.99	2.46
w <i>R</i> 2 (all data) (%)	7.57	6.97	4.33	5.43
GOF on <i>F</i> ²	0.86	0.97	0.89	0.91
$\Delta\rho$ (e Å ⁻³)	0.35, –0.25	1.58, –0.87	0.70, –0.66	0.98, –0.61

the hafnocene alkyne complex Cp₂Hf(HMe₂SiC₂SiMe₂H). We performed additional NMR measurements at room temperature of the mixture that was heated to 110 °C for 40 min, and we have observed an analogous composition of the mixture, while the Cp signal appeared as a broad signal at 4.86 ppm and the Si–H signal moved slightly to –4.09 ppm. Unfortunately, in the ²⁹Si spectra, we were not able to find corresponding signals, possibly due to certain broadening, which did not allow us to unambiguously prove the presence of the suggested intermediates.

While compounds **16** and **19** clearly represented the preferred structure type for alkynes **5** and **18**, respectively, the unsymmetrical alkyne **1** did not give such products. Presumably, the steric bulk of one SiMe₃ group precludes the formation of the corresponding metallacycle, as is possible in the presence of two less sterically demanding SiMe₂H or SiPhH₂ groups. We can speculate that the insertion step to the Hf–Si bond is impossible for this substrate, while the intermediate alkyne complex is not sufficiently stable to be isolated.

4. Computational Analysis

Along with the experimental investigations we carried out density functional theory calculations for understanding the reaction mechanism proposed in Scheme 7. Instead of the substituted alkynylsilane substrates, we used the parent H₃SiC₂SiH₃ as a model substrate. This model is appropriate, since both alkynylsilanes **5** and **18** formed the same structure pattern in products. In our discussion we have used the lettering system **A–D**, conformable with the previous usage (Scheme 7), for the stationary points on the potential energy surface (Schemes 8 and 9).

As proposed in Scheme 7, the reaction has two basic steps toward the formation of products: (1) the formation of the alkyne complex **A** along with its isomerization to the corresponding silene complex **C** (cf. Scheme 8, structures **A1–C3**), and (2) the selective insertion of the second alkyne molecule to afford

the final product (represented by **D1** in Scheme 9). The origin of the presented energetic values is **A1** and H₃SiC₂SiH₃ as the substrate.

A1 is more stable than the corresponding hafnocene alkyne complex without the agostic interaction (having a *cis* configuration of the coordinated alkyne), which is in agreement with the behavior of the corresponding Ti and Zr complexes from the review of both experiments²² and computations (see ref 23 and the Supporting Information). However, we could not find the corresponding intermediate with the broken H–Si bond, and optimizations for this species led back to **A1**, which can be explained by the charge separation between the negatively charged hydride and the positively charged SiH₂ group. In addition, attempts to locate the corresponding species with only H–Si bond coordination leading to an oxidative addition resulted in the structure **B1**, which is higher in energy than **A1** by 10.93 kcal/mol. Such hafnocene silyl hydride complexes have been described, and the observed structural parameters for Cp*₂Hf(H)[SiH(SiMe₃)₂] (Hf–Si = 2.744(1) Å),^{13c} the solid-state structure of which was determined, correspond with our model. However, we also could not find the corresponding transition state from **A1** to **B1**, and this process can be considered as the only energy-raising process. The next step from **B1** to **B2** can be considered as the coordination of the silapropargyl moiety of **B1**, while **B2** is higher in energy than **A1** by 5.69 kcal/mol. It is interesting to note that **B2** has hydride and silaallenyl coordination and can be considered as a rotational isomer of **A1** by rotating the silaallene group by approximately 180°.

The next step is a hydride transfer from **B2** through the transition state **B3-TS** to **C1**; the computed barrier of 2.47 kcal/mol for this process is rather low. An agostic C–H–Hf interaction is present in **C1**. The subsequent step is the breaking of this agostic interaction and the bending out of the vinyl group (through the transition state **C2-TS**), resulting in the formation of a silene complex (**C3**). As shown in Scheme 8, the transformation from **A1** to **C3** raises the energy by only 5.58

kcal/mol and the single step with the highest energy is about 11 kcal/mol. All this indicates a slightly endogenic process with moderate energy barriers.

Postulating the formation of silene complex **C3**, we were furthermore interested in the selective insertion of a second alkyne molecule leading to the corresponding products. As shown in **C3**, there are two possibilities for the alkyne insertion: one into the Hf–Si bond and the other into the Hf–C bond. It should be noted that the insertion process into both Hf–Si and Hf–C bonds is a single-step process leading directly to the product and does not form any intermediates as a stepwise process. As shown in Scheme 9, the insertion into the Hf–Si bond via **C4-TS-1** has an activation free energy lower than that into the Hf–C bond via **C4-TS-2** (27.79 vs 31.25 kcal/mol), while the corresponding insertion product **D2** is more stable than **D1** (–13.96 vs –12.72 kcal/mol). The difference (3.46 kcal/mol) in activation free energy confirms the selective formation of **D1**, as found experimentally (Scheme 7), and the process is kinetically controlled. The enhanced thermodynamic stability of **D2** over **D1** is due to the formation of an additional agostic interaction. Calculated structural parameters for the product **D1** are in good agreement with the experimentally obtained values for both **16** (Figure 3) and **19** (Figure 4).

5. Conclusions

We have demonstrated a diversity in the behavior of alkynylsilanes in reactions with metallocene alkyl complexes as well as with in situ generated “free” metallocenes. Depending on the metal, substituents of the metallocene precursor, and substituents on the alkyne, respectively, different product types were formed. Processes during these reactions include the Si–H bond activation of the silane that subsequently facilitates the creation of new Si–C bonds. On the other hand, interaction of the alkyne with the metallocene core is an important phenomenon. In reactions with alkynylsilanes, Ti and Zr obviously preferred the alkyne coordination. Metallocene alkyne complexes were thus obtained, some of which were synthesized previously in a different manner. Nevertheless, the typical feature of the reactions utilizing Cp_2TiMe_2 was methyl group transfer to the Si atom, which unequivocally demonstrates the previous Si–H bond activation.³⁸ When the $\text{Cp}_2\text{MCl}_2/n\text{-BuLi}$ ($\text{M} = \text{Ti}, \text{Zr}$) systems were used, an analogous transfer of *n*-butyl groups was detected only in the case of Zr. This process, however, can also be viewed as a hydrosilylation reaction, since the presence of metallocene alkene complexes can be anticipated under such reaction conditions.³⁹ It should be noted that the $\text{Cp}_2\text{ZrCl}_2/n\text{-BuLi}$ system yielded inseparable mixtures of products and therefore turned out to be an inconvenient “ Cp_2Zr ” source in this particular case in comparison to the $\text{Cp}_2\text{ZrCl}_2/\text{Mg}$ system.²²

In contrast to Ti and Zr, Hf preferred the formation of metallacycles in most cases. However, steric features of the substituents on the alkyne substrate played a key role and, in some cases, *n*-butyl group transfer to Si was also observed. The less sterically demanding alkyne **12** facilitated the coupling of two substrate molecules to give exclusively hafnacyclopentadienes as known types of products. In the case of alkyne **1**, the

steric bulk of the SiMe_3 group prevented the formation of metallacyclic products from two alkyne molecules. The hafnocene alkyne complex of **1** was isolable only after utilizing the additional stabilizing PMe_3 ligand. On the other hand, symmetrical alkynes **5** and **18** provided novel five-membered Hf- and Si-containing metallacycles with an exocyclic double bond (**16** and **19**, respectively). DFT calculations confirmed the plausibility of the proposed intermediates and some of the elementary steps in the suggested mechanism of their formation. The latter type of reactivity revealed, in comparison to Ti and Zr, a significant difference in the hafnium chemistry arising from the possible exceptional rearrangement after the Si–H bond activation in alkynylsilanes.

6. Experimental Section

6.1. General Considerations. All manipulations were carried out under an atmosphere of argon using standard Schlenk techniques. Prior to use, solvents (including deuterated) were predried, freshly distilled from sodium tetraethylaluminate, and stored under argon. Cp_2MCl_2 ($\text{M} = \text{Ti}, \text{Zr}, \text{Hf}$) and Cp_2TiMe_2 (5% solution in toluene) were purchased from MCAT (Metallocene Catalysts & Life Science Technologies, Konstanz, Germany). Alkyne **12** was purchased from ABCR. Cp_2ZrMe_2 ,⁴⁰ $\text{Cp}_2\text{Hf}(n\text{-Bu})_2$,^{4b} and alkynes **1**,^{41a} **2**,^{41a} **5**,^{41b} and **18**³³ were synthesized according to published procedures. The following instruments were used. NMR: Bruker AV 400 and AV 300 spectrometers were used; chemical shifts (^1H , ^{13}C , ^{29}Si) are given relative to SiMe_4 and are referenced to residual solvent signals (benzene- d_6 , δ_{H} 7.16, δ_{C} 128.0; toluene- d_8 , δ_{H} 2.03, δ_{C} 20.4; THF- d_8 , δ_{H} 1.73, δ_{C} 25.2). Where necessary, signals were assigned with the aid of 2D NMR experiments: COSY, HMQC, HMBC, NOESY. MS: MAT 95-XP (EI- and CI-MS) and Agilent Technologies 6210 (TOF LC-MS) and 6890N+5973N (GC-MS). IR: Bruker Alpha-P. Elemental analyses: Leco TruSpec Micro CHNS. Melting points: Büchi 535 apparatus, capillaries sealed under Ar.

6.2. X-ray Structure Determination. Crystals suitable for measurement were obtained from *n*-hexane at -40°C (**4**), by slow evaporation of an *n*-hexane solution (**11** and **19**) or benzene- d_6 solution (**16**) under a stream of argon. Diffraction data were collected on a STOE IPDS II diffractometer using graphite-monochromated $\text{Mo K}\alpha$ radiation. The structures were solved by direct methods (SHELXS-97⁴²) and refined by full-matrix least-squares techniques on F^2 (SHELXL-97⁴²). For all compounds a numerical absorption correction was applied. For compound **11**, both Cp rings in the structure were treated as rigid groups and the disordered SiMe_3 group was modeled over two positions. The structures of compounds **16** and **19** contained two disordered cyclopentadienyl ligands. For **16**, each of them was successfully modeled over two positions. In the case of **19**, one was treated as a rigid group (C29–C33), while the other was modeled over two positions (C34–C38). All fully occupied non-hydrogen atoms were refined anisotropically. Hydrogen atoms (except H1 of compound **11**, H1, H2, H4A, and H4B of **16**, and H1A, H1B, H2A, H2B, H3, H4B, and H4C of **19**, which were located in the difference map) are placed in idealized positions and refined using a riding model. The DIAMOND⁴³ program was used for graphical representations. Crystallographic data for compounds **4**, **11**, **16**, and **19** are given in Table 1.

(38) A similar methyl transfer process from Cp_2TiMe_2 to silanes was briefly mentioned in the studies of Harrod and co-workers.^{11b,18}

(39) We are aware of the fact that such an explanation is speculative. Notably, the decomposition of $\text{Cp}_2\text{Zr}(n\text{-Bu})_2$ was shown upon detailed analysis to be a complicated set of reactions rather than simple elimination of butane and the formation of a butene complex.²⁹

(40) Wailes, P. C.; Weigold, H.; Bell, A. P. *J. Organomet. Chem.* **1972**, *34*, 155.

(41) (a) Ruffolo, R.; Decken, A.; Girard, L.; Gupta, H. K.; Brook, M. A.; McGlinchey, M. J. *Organometallics* **1994**, *13*, 4328. (b) Wrackmeyer, B.;kehr, G.; Süß, J.; Molla, E. *J. Organomet. Chem.* **1998**, *562*, 207.

(42) Sheldrick, G. M. *Acta Crystallogr.* **2008**, *A64*, 112.

(43) Brandenburg, K. DIAMOND, Version 3.1e; Crystal Impact GbR, Bonn, Germany, 2007.

6.3. Reactions of Cp₂TiMe₂ with Alkynylsilanes: General

Procedure. A commercial 5% toluene solution (3.0 mL) of Cp₂TiMe₂ was evaporated to dryness in the dark, and the solid (145 mg, 0.70 mmol) was dissolved in *n*-hexane (10 mL). The corresponding alkyne (0.77 mmol) was introduced, and the resulting orange solution was heated to reflux for 1.5 h, during which time the color changed to dark amber. After it was cooled to room temperature, the solution was evaporated under vacuum, the solid residue extracted with *n*-hexane (all solids were readily soluble), the extract filtered, and the solvent removed in vacuo, leaving an amber solid.

Thus, the reaction of alkyne **1** afforded complex **3** of >90% purity in virtually quantitative yield, while the reaction of **5** yielded a mixture of **3** and **6** in a ca. 1:1 ratio, together with some minor unidentified compounds (up to 10 mol %). The reaction products were not further purified. NMR data for complexes **3**^{2c} and **6**^{4b} were in agreement with those previously reported. Compound **4** was recrystallized from *n*-hexane at –40 °C to give dark amber crystals. Yield: 208 mg (63%). Mp: 118–120 °C dec. Anal. Calcd for C₂₈H₃₂Si₂Ti (472.59 g mol⁻¹): C, 71.16; H, 6.83. Found: C, 71.04; H, 7.04. NMR (400 MHz, 297 K, benzene-*d*₆): ¹H, δ –0.36 (s, 9 H, SiMe₃), 0.11 (s, 3 H, SiMePh₂), 6.35 (s, 10 H, C₅H₅), 7.12–7.25 (m, 10 H, SiMePh₂); ¹³C{¹H}, δ –1.4 (SiMePh₂), 0.4 (SiMe₃), 117.8 (C₅H₅), 127.9, 129.2, 134.8 (3 × SiMePh₂ CH), 138.4 (SiMePh₂ C_{ipso}), 236.0 (CSiPh₂Me), 248.2 (CSiMe₃); ²⁹Si{¹H}, δ –21.9 (SiPh₂Me), –14.3 (SiMe₃). IR (Nujol): $\tilde{\nu}/\text{cm}^{-1}$ 1648 (m, C≡C). MS (CI, isobutane): *m/z* 472 [M]⁺, 295 [Me₃SiC₂SiMe₂C₅H₆N + H]⁺.

6.4. Reaction of the Cp₂TiCl₂/*n*-BuLi System with Alkynes **1 and **5**.** A solution of Cp₂TiCl₂ (100 mg, 0.40 mmol) in THF (10 mL) was cooled in a dry ice–ethanol bath to –78 °C, and *n*-BuLi (0.50 mL of 1.6 M solution in hexanes, 0.80 mmol) was slowly introduced. After the mixture was stirred for 10 min at –78 °C, the alkyne **1** (70 mg, 0.45 mmol) was added to the deep red mixture, which was then warmed slowly to room temperature and stirred for 3 h, while the color changed to dark brown. All volatiles were evaporated under vacuum, and the residue was extracted with *n*-hexane (15 mL). Removal of the solvent afforded a dark amber residue, which was identified by NMR as complex **6** accompanied by some minor unidentified byproducts (up to 10 mol %).

In the same manner, the reaction utilizing alkyne **5** (63 mg, 0.44 mmol) yielded compound **7** (purity varied between ca. 80 and 90%). Compounds **6** and **7** were identified by the comparison of NMR spectra with previously published data.^{22b} Owing to the high solubility of impurities as well as **6** and **7**, and their reluctance to crystallize under such conditions, the reaction products could not be isolated in a pure state.

6.5. Preparation of Complex 16. Method a. Alkyne **5** (252 mg, 1.77 mmol) was added to a solution of Cp₂Hf(*n*-Bu)₂ (250 mg, 0.59 mmol) in toluene (15 mL) at room temperature. The mixture was heated to 110 °C for 7 h. After the mixture was cooled to room temperature, all volatiles were removed under vacuum to leave an orange solid, which was identified as compound **16** of ca. 95% purity, contaminated only by traces of **17**. Yield: 309 mg (88%). The product can be further recrystallized from a concentrated *n*-hexane solution at –78 °C.

Method b. Cp₂HfCl₂ (150 mg, 0.40 mmol), alkyne **5** (145 mg, 1.02 mmol), and magnesium turnings (10 mg, 0.41 mmol) were suspended in THF (10 mL), and the mixture was heated to 60 °C and stirred for 5 days at this temperature, during which time the color changed from pale yellow to dark amber. After the mixture was cooled to room temperature, all volatiles were evaporated and the residue was extracted with *n*-hexane (2 × 10 mL). Removal of the solvent from extracts afforded 167 mg (70%) of **16** with a purity similar to that in the previous case. Characterization data for **16** are as follows. Mp: 140–141 °C dec. Anal. Calcd for C₂₂H₃₈HfSi₄ (593.37 g mol⁻¹): C, 44.53; H, 6.45. Found: C, 44.58; H, 6.45. NMR (400 MHz, 297 K, benzene-*d*₆; numbering according to atom labeling in the molecular structure, see Figure 3): ¹H, δ 0.22 (d,

³J_{HH} = 3.6 Hz, 6 H, Me₂ at Si4), 0.28 (d, ³J_{HH} = 3.8 Hz, 6 H, Me₂ at Si2), 0.37 (d, ³J_{HH} = 3.8 Hz, 6 H, Me₂ at Si1), 0.47 (s, 6 H, Me₂ at Si3), 3.80 (hept, ³J_{HH} = 3.8 Hz, 1 H, Si1–H), 4.37 (hept, ³J_{HH} = 3.8 Hz, 1 H, Si2–H, and dhept, ³J_{HH} = 3.6, and 7.1 Hz, 1 H, Si4–H), 5.78 (s, 10 H, C₅H₅), 7.31 (d, ³J_{HH} = 7.1 Hz, 1 H, C4–H); ¹³C{¹H}, δ –2.9 (Me at Si4₂), –0.4 (Me₂ at Si2), –0.3 (Me₂ at Si1), 2.5 (Me₂ at Si3), 111.2 (C₅H₅), 159.8 (C4), 179.7 (C2), 244.6 (C3), 263.4 (C1); ²⁹Si{¹H}, δ –52.7 (Si3), –40.5 (¹J_{SiH} = 171 Hz, Si1), –30.0 (¹J_{SiH} = 185 Hz, Si4), –23.3 (¹J_{SiH} = 182 Hz, Si2). IR (Nujol): $\tilde{\nu}/\text{cm}^{-1}$ 2137, 2115, 2080 (3 × m, Si–H). MS (CI, isobutane): *m/z* 594 [M]⁺, 283 [C₁₂H₂₇Si₄]⁺.

6.6. Preparation of Complex rac-19. Method a. In an analogy to the preparation of **16**, alkyne **18** (169 mg, 0.71 mmol) and Cp₂Hf(*n*-Bu)₂ (100 mg, 0.24 mmol) were reacted in toluene (10 mL). Crude compound **19** was isolated as an orange solid contaminated with **18**. The crystalline **19** was subsequently washed with *n*-pentane to remove the impurities. Yield: 159 mg (84%).

Method b. According to the same procedure as for **16**, Cp₂HfCl₂ (190 mg, 0.50 mmol), alkyne **18** (358 mg, 1.50 mmol), and magnesium turnings (13 mg, 0.53 mmol) reacted in THF (10 mL) at 60 °C for 2 days to give the crude crystalline **19** contaminated with **18**, which was treated in the same manner as above or recrystallized from *n*-hexane at –78 °C. Yield: 251 mg (64%). Mp: 130–131 °C. Anal. Calcd for C₃₈H₃₈HfSi₄ (785.54 g mol⁻¹): C, 58.10; H, 4.88. Found: C, 58.10; H, 5.16. NMR (400 MHz, 297 K, benzene-*d*₆; numbering according to atom labeling in the molecular structure, see Figure 4): ¹H, δ 4.66 (dd, ²J_{HH} = 5.7 Hz, ³J_{HH} = 3.9 Hz, 1 H, Si4–H), 4.78 (d, ²J_{HH} = 5.5 Hz, 1 H, Si1–H), 4.85 (dd, ²J_{HH} = 5.7 Hz, ³J_{HH} = 4.7 Hz, 1 H, Si4–H), 4.95 (d, ²J_{HH} = 5.8 Hz, 1 H, Si2–H), 4.98 (d, ²J_{HH} = 5.5 Hz, 1 H, Si1–H), 5.07 (d, ²J_{HH} = 5.8 Hz, 1 H, Si2–H), 5.40 (d, ⁴J_{HH} = 1.4 Hz, 1 H, Si3–H), 5.73, 5.76 (2 × s, 10 H, C₅H₅), 7.55 (ddd, ³J_{HH} = 3.9 and 4.7 Hz, ⁴J_{HH} = 1.4 Hz, 1 H, C4–H), 7.03–7.88 (m, 20 H, Ph); ¹³C{¹H}, δ 111.6, 112.2 (2 × C₅H₅), 128.1, 128.3, 128.5, 129.4, 129.6, 129.8, 133.6, 133.7, 135.7, 136.2, 136.6, 136.8 (12 × Ph), 157.4 (C4), 171.9 (C2), 242.4 (C3), 263.0 (C1), signals of four Ph groups in the range between 128.0 and 137.0 are partially overlapped and are not unambiguously assigned; ²⁹Si{¹H}, δ –65.7 (Si3), –55.9 (Si1), –50.4 (Si4), –47.9 (Si2). IR (Nujol): $\tilde{\nu}/\text{cm}^{-1}$ 2145, 2125 (2 × m, Si–H), 2092 (s, Si–H), 2065 (m, Si–H). MS (CI, isobutane): *m/z* 785 [M]⁺.

6.7. Computational Details. Our computations have been carried out at the BP86 level of density functional theory as implemented in the Gaussian 03 program.⁴⁴ We have used the standard 6-311+G(d,p) basis set for H, C, and Si atoms and the LANL2DZ basis set for Ti, Zr, and Hf.⁴⁵ All structures have been optimized in C₁ symmetry without any constraints, and all optimized structures have been characterized either as energy minima without imaginary frequencies or as transition states with only one imaginary frequency by frequency calculations at the same level. For discussion we have used the computed Gibbs free energies (ΔG) at 298 K and the computed enthalpies (ΔH, 298 K) that are given for comparison. For comparison we have also carried out MP2 single-point energy calculations by using the same basis sets and the BP86 optimized geometries.

Our benchmark calculations on the acetylene complex with and without H–Si agostic interactions show that BP86 not only reproduces structural parameters very well but also gives the correct relative energies; i.e., BP86 favors the structure with an agostic interaction by ΔG = –4.01 kcal/mol (ΔH = –4.92 kcal/mol) for M = Zr and ΔG = –3.06 kcal/mol (ΔH = –3.55 kcal/mol) for M = Hf. However, for M = Ti, the structure with an agostic interaction is less stable by ΔG = 3.33 kcal/mol (ΔH = –0.08 kcal/mol, indicating the entropy effect). MP2 single-point energy calculations including the thermal correction to Gibbs free energy give the correct energetic order; i.e., the structure with an agostic interaction

(44) Frisch, M. J. et al.; *Gaussian 03*, Revision D.01; Gaussian, Inc.: Wallingford, CT, 2004.

(45) Hay, P. J.; Wadt, W. R. *J. Chem. Phys.* **1985**, *82*, 299.

is more stable by $\Delta G = 1.24$ kcal/mol for Ti, $\Delta G = 7.37$ kcal/mol for Zr, and $\Delta G = 5.58$ kcal/mol for M = Hf.

In addition, we have also done all calculations by using the well-accepted B3LYP method with the same basis set. B3LYP can reproduce the geometric parameters but gives the opposite order of stability; i.e., B3LYP favors the structure without an agostic interaction by $\Delta G = 7.29$ kcal/mol ($\Delta H = 6.66$ kcal/mol) for M = Ti, $\Delta G = 0.73$ kcal/mol ($\Delta H = 0.67$ kcal/mol) for M = Zr, and $\Delta G = 2.44$ kcal/mol ($\Delta H = 2.19$ kcal/mol) for M = Hf.

On the basis of these energetic data, the energy difference between two structural forms should not be too large; we have used the BP86 method for our calculations, and the MP2 energetic data are included. All these data are listed in the Supporting Information.

Acknowledgment. This work is dedicated to Prof. Dietmar Seyferth in appreciation of his advancement of the area of organometallic chemistry. We thank our technical staff, in particular

Regina Jesse, for assistance. This work was supported by the Deutsche Forschungsgemeinschaft (Project No. GRK 1213).

Supporting Information Available: Text and tables giving synthetic procedures for compounds **10**, **11**, **13–15**, and **17** along with their characterization data, experimental procedures for reactions of the $\text{Cp}_2\text{ZrCl}_2/n\text{-BuLi}$ system with alkynes **1** and **5** and of hafnocene precursors with alkyne **1**, all computational details (benchmark calculations, electronic energies, computed Cartesian coordinates, and selected structural parameters), Si–Si and Si–C coupling constants for **4**, **14**, **16**, and **19**, complete ref 44, and CIF files giving crystallographic data for **4**, **11**, **16**, and *rac*-**19**. This material is available free of charge via the Internet at <http://pubs.acs.org>.

JA910527W